

NATIONAL TRANSPORTATION SAFETY BOARD



Office of Research and Engineering
Vehicle Performance Division
Washington, D.C. 20594

October 6, 2000

ACCIDENT RECONSTRUCTION STUDY: BIOMECHANICS

By: Kristin M. Bolte, Ph.D.

ACCIDENT:

Location: Intersection of State Route 30A and State Route 7; Schoharie County, Central Bridge, NY
Date: October 21, 1999
Time: 10:30 a.m., Local Time
Vehicle 1: 1997 International AmTran 66 Passenger School Bus
Vehicle 2: 1987 Mack Tandem Axle Dump Truck, 1988 Interstate Utility Trailer
NTSB #: HWY-00-FH-001

GROUP

Kristin Bolte, Ph.D.,	Group Chairman,	NTSB Washington, D.C.
Michele McDonald, MFS,	Group Member,	NTSB Washington, D.C.
Henry Hughes,	Group Member,	NTSB Washington, D.C.
Lawrence Jackson, MS, PE,	Group Member,	NTSB Washington, D.C.
Shane Lack,	Group Member,	NTSB Washington, D.C.

SUMMARY

Accident Synopsis

On Thursday, October 21, 1999, at about 10:30 a.m. EDT a 1997 International AmTran school bus, operated by Kinnicutt Bus Company, was northbound on State Route 30A (SR-30A/Zicha Road). The bus, occupied by the driver, 44 students (ages 5 to 9), and eight adults, was en-route to an Albany City School field activity. The bus drove past the dual flashing red signals and stop sign at the intersection of SR-30A and State Route 7 (SR-7) into the path of an oncoming westbound 1987 Mack dump truck towing a utility trailer, operated by MVF Construction Company. Five students and two adults were seriously injured, about 30 students, one adult, and both drivers sustained minor injuries, and nine students and three adults were uninjured.

At impact, the front of the dump truck contacted the right side of the school bus behind the rear wheel. The bus and dump truck both began to rotate clockwise, as seen from above. The bus ended up facing the impact region, backed into the adjacent field. The dump truck impacted three signs and a metal traffic signal on the side of the road and came to rest next to the pole.

Figure 1 shows a picture of the final rest positions of the school bus and the dump truck. The exterior damage to the bus and the location of the major impact forces can be seen in Figure 2.

Contents of this study

Purpose

This study was conducted to determine possible occupant kinematics based on the severity of the crash and the developed crash forces. Two areas of the school bus were examined for this study. The first area for this study was the second to last row of the school bus on the passenger side of the bus. This was the area of maximum intrusion and also of the most severe injuries. Three passengers were seated in this row on the passenger side of the bus: one reportedly unrestrained chaperone, and two 7-year-old reportedly lap belt restrained students. Occupant kinematics were investigated for a variety of scenarios. The first scenario looked at the reported restraint condition at the time of the accident: two lap-belt restrained 7 year-old females and one unrestrained adult male. The second scenario investigated the condition of having all three occupants unrestrained. The third condition investigated having all three occupants lap-belt restrained and the fourth investigated having all three restrained with lap/shoulder belt. The final scenario investigated the occupant kinematics and predicted injuries given an unrestrained and a lap-belt restrained condition for the two simulated females but without the adult male included in the simulation.

The second area for this study was row 5 on the driver's side of this bus. This row was the row containing the flip seat that was adjacent to the side emergency exit door. Occupant kinematics in the area of the side emergency exit door were investigated to determine if contact between the simulated occupant and the unprotected surfaces of the side emergency exit door occurred during either the initial occupant impact or subsequent occupant impacts. Both the unrestrained and lap belted conditions were simulated.

Tools

The interaction between the school bus and the dump truck was simulated using the "EDSMAC4" software, developed by Engineering Dynamics Corporation, and is further detailed in the Accident Reconstruction Study.

Another software program, Graphical Articulated Total Body (GATB)¹, developed by Collision Engineering Associates for the HVE system, was used to model the occupant kinematics. This program calculates the unrestricted motion of all 15 rigid segments of the body and the resulting forces due to the interactions of these segments with the contact surfaces defined in the vehicle. The GATB models are constructed using the HVE Human Model. The HVE Human Model is a mathematical model based on the regression equations predicting the dimensions and the inertial properties of each human segment calculated from the anthropometry of children, youths, and adults.^{2,3,4} These equations are grouped into a program developed at Wright-Patterson Air Force Base called Generator of Body Data (GEBOD).⁵

This study will describe the programs implemented to study the occupant kinematics, and the resulting forces and potential injury causing mechanisms. It will describe the inputs, the outputs, and the resulting visualizations of the simulations. The vehicle dynamics, although briefly discussed in this report, are more thoroughly addressed in the Accident Reconstruction Study, separate from this report.

SCHOOL BUS DYNAMICS

The dynamics of the school bus were calculated using the three-dimensional software program, HVE (using EDSMAC4). The details of the HVE studies are provided in the Accident Reconstruction Study.

Coordinate System

The coordinate system of the vehicle, established by HVE, was such that the positive x-axis pointed toward the front of the vehicle. The positive y-axis pointed toward the right side of the vehicle and the positive z-axis pointed downward toward the bottom of the vehicle.

¹ Grimes, W.D. "Using ATB Under the HVE Environment", SAE 970967, 1997.

² Snyder, R.G., Schneider, L.W., Owings, C.L., Reynolds, H.M., Golomb, D.H., Sckork, M.A., May 1977, *Anthropometry of Infants, Children, and Youths to Age 18 for Product Safety Design*, UM-HSRI-77-17, Consumer Product Safety Commission, Bethesda, MD.

³ Grunhofer, H.J., Kroh, G., 1975, *A Review of Anthropometric Data on German Air Force and United States Air Force Flying Personnel 1967-1968*, AGARD-AG-205 (AD A010 674), Advisory Group for Aerospace Research and Development, 7 Rue Ancelle 92200, Neuilly Sur Seine, France.

⁴ McConville, J.T., Churchill, T.D., Kaleps, I., Clauser, C.E., Cuzzi, J., 1980, *Anthropometric Relationships of Body and Body Segment Moments of Inertia*, AMRL-TR-80-119 (AD A097 238), Aerospace Medical Research Laboratory, Wright-Patterson Air Force Base, Ohio.

⁵ Cheng, H, Obergefell, L, Rizer, A. *Generator of Body Data (GEBOD) Manual*, AL/CF-TR-1994-0051, Systems Research Laboratories, Inc. Dayton, OH, 1994.

GATB Pulse

The position-time history for the school bus was referenced to the center of gravity of the bus. Occupant motion was calculated based on the distance of the occupant from the center of gravity. Graphs showing the linear and angular position-time history of the bus as calculated in the Accident Reconstruction Study are shown in Figure 3. (Note that EDSMAC4 is a two-dimensional program and therefore the position and orientation are shown in two dimensions.)

It is important to note that this position-time history was not the exact displacement that the vehicle experienced during the accident, but was representative of the crash based on the input assumptions in HVE. The GATB simulation therefore used the position-time history to simulate the dynamics of the bus during the collision.

The position-time history output from EDSMAC4 was slightly altered for input into GATB. The EDSMAC4 collision algorithm is two-dimensional. Therefore, changes in the vertical position were only due to the changes in elevation along the roadway. The spline algorithm⁶ used in GATB fits a curve through the position data in order to calculate the velocity and the acceleration. Although the vertical position magnitude measurements were small, the changes in magnitude resulted in large accelerations that were erroneous due to the derivative process. Therefore, the z-component of the position-time history was set to a constant value.

Deformations

The school bus was subjected to a side impact collision with the dump truck pulling an Interstate utility trailer. The impact occurred on the passenger's side of the bus near the second to last row of the school bus. At impact, both the bus and the dump truck began to rotate clockwise, as seen from above. The majority of the damage was located on the passenger's side of the bus near the last rows of the school bus. (See Figure 4a and Figure 4b)

SCHOOL BUS OCCUPANT BIOMECHANICS

The biomechanics of the occupants were investigated using GATB. Occupant kinematics follow the laws of physics. An occupant in a vehicle traveling at a constant speed typically has little or no velocity relative to the vehicle within which he or she is traveling. When an accident occurs, the vehicle may decelerate (or accelerate) rapidly due to the impact with another object. During the accident, the occupant continues in the same path and at the same velocity as the vehicle was traveling before the accident until the occupant comes in contact with an object inside the vehicle. (In most simulation programs, an occupant is considered to be in contact with another surface when some part of the occupant's body occupies the same space as a defined surface in the vehicle.) This contact may be with a seat belt, an air bag, the seat

⁶ A spline algorithm fits a curve between data points.

back in front of the occupant, or any other surface in the vehicle. Importantly, the vehicle will have decreased (or increased) in speed due to the impact and thus, the occupant will strike the surface inside of the vehicle because the occupant is traveling faster (or slower) than the vehicle.

The time between when the vehicle starts to decelerate (or accelerate) and when the occupant first contacts something inside the vehicle is critical. If the occupant first contacts a well-fitted seat belt, there will be little velocity difference between the vehicle and the portion of the occupant restrained by the belt because the occupant did not travel far to first contact the belt. Other portions of the occupant such as the head and extremities will experience a greater velocity difference. If the occupant travels a greater distance before contacting a surface inside of the vehicle, such as the steering wheel, the dash board, or the seat in front of the occupant, the velocity difference between the vehicle and the occupant will be much greater because the vehicle will have had more time to decelerate (or accelerate) while the occupant has not yet experienced a force to cause deceleration (or acceleration). If the velocity difference is great, the force on the occupant will be much more severe than if the velocity difference is small.⁷ In addition, if the occupant contacts the inside of the vehicle relatively early in the crash, the occupant is able to decelerate (or accelerate) with the vehicle and can take advantage of all the energy absorbed by the vehicle during the later portion of the crash. This gradual slowing of the vehicle is commonly referred to as the 'ride down'.

Simulations of occupant kinematics involve three stages. The first stage is to define the motion of the vehicle or the crash pulse. This information gives the acceleration-time history or the position-time history of the vehicle at the center of gravity of the vehicle. The second stage involves placing the occupant within the vehicle. The occupant must be in equilibrium in the seated position and therefore must not have residual forces acting on the joints of the body.⁸ Placing the occupant in the vehicle also includes defining the surfaces within the vehicle that may be contacted by the occupant during the crash. These surfaces include the seat cushion, seat back, the restraint system, the steering wheel, the windows, the windshield, and any other potential contact surface. The third stage involves driving the vehicle through its accident trajectory and calculating the direction and duration of occupant contacts with different surfaces inside the vehicle. Potential injuries to the occupant may be suggested based on the magnitude and duration of the forces acting on the occupant from the contact surfaces, the accelerations of the body, and the anatomy/physiology of the occupant.

⁷ In a school bus, the seats are designed such that the unrestrained occupant during a frontal collision contacts the seat backs with a large portion of their body, distributing the forces over a larger surface area.

⁸ The occupant kinematics software acts to move the person such that the internal forces on the body are approximately zero.

Injury Criteria

There are several measures of injury severity currently used to predict injury. Additional measures have recently been proposed by the NHTSA. A summary of most of these measures is provided here.

The head injury criteria (HIC) was developed from a variety of research studies predicting injury from peak acceleration, pulse duration, and concussion onset. The Wayne State Tolerance Curve (WSTC) was developed to relate the acceleration of the head to the risk of skull fracture and was first presented by Lissner in 1960.⁹ Later work by Gadd (1966)¹⁰ provided an index, the Gadd Severity Index (GSI), which combined the data of the WSTC with tolerance data. The HIC was first proposed by Versace in 1971¹¹ and was later modified by the National Highway Traffic Safety Administration (NHTSA). The equation for calculating HIC is as follows:

$$HIC = \max \left[\frac{1}{t_2 - t_1} \int_{t_1}^{t_2} a(t) dt \right]^{2.5} (t_2 - t_1)$$

The current critical HIC value for the mid-sized male simulated occupant for frontal protection is 1000.¹² It is important to note that research concerning injuries to children in vehicle accidents is limited. Therefore, various scaling techniques, based on geometric and material scaling and engineering judgement, were used by NHTSA to determine the HIC values for the other sized dummies resulting in a NHTSA proposed critical HIC value for the 5th percentile female simulated occupant and the 6-year-old simulated occupant of 1000. The NHTSA proposed critical HIC value for the 3-year-old simulated occupant is 900.

In the past, the thoracic injury criteria had been measured by the chest acceleration and chest deflection with maximum values of 60 G's and 3 inches, for the 50th percentile adult male. (The maximum chest deflection was reduced to 2.5 inches for the 5th percentile female, 1.9 inches for the 6-year-old child, and 1.7 inches (and 50 G's) for the 3-year-old child dummy.) A recent NPRM by the NHTSA¹² indicates that a combination of both chest acceleration and

⁹ Lissner HR, Lebow M, Evans FG. Experimental Studies on the Relation Between Acceleration and Intracranial Pressure Changes in Man. *Surgery, Gynecology, and Obstetrics*, Volume III, p. 329-338, 1960.

¹⁰ Gadd CW. Use of a Weighted-Impulse Criterion for Estimating Injury Hazard. *Proceedings of the Tenth Stapp Car Crash Conference*, SAE Paper 660793, 1966.

¹¹ Versace J. A Review of the severity Index. *Proceedings of the Fifteenth Stapp Car Crash Conference*, SAE Paper 710881, 1971.

¹² Kleinberger M, Sun E, Eppinger R, et al. Development of Improved Injury Criteria for the Assessment of Advanced Automotive Restraint Systems, NHTSA, September 1998.

chest deflection are predictive of thoracic injury, based on the linear combination of the thoracic spine resultant acceleration and the maximum chest deflection. This equation is termed the Combined Thoracic Index (CTI) with a critical value of 1.0 and is defined below.

$$CTI = \frac{A_{\max}}{A_{\text{int}}} + \frac{D_{\max}}{D_{\text{int}}}$$

where A_{\max} is the maximum value of a 3 milli-second spinal acceleration clip and D_{\max} is the maximum value of the dummy chest deflection. A_{int} and D_{int} are set by the 50% probability of injury line and are the horizontal and vertical intercepts of this line. The values for A_{int} and D_{int} are 85 G and 102 mm, respectively for the mid-sized adult male. In order to pass the NHTSA proposed criteria (i.e. for the occupant to have an AIS¹³ < 3), all three limits: maximum chest acceleration < 60 G's, maximum chest deflection < 3 inches, and CTI < 1.0, must be satisfied.

The current tolerance limits in FMVSS No. 208 detail the limits for compression (4000 N), tension (3300 N), shear (3000 N), flexion moment (190 Nm), and extension moment (57 Nm) of the neck, individually. These measures do not address the combined effects of two loading modes, for example flexion and tension. In 1984, Prasad and Daniel¹⁴ introduced the idea that a neck injury indicator should be based on a linear combination of axial loads and bending moments. This concept was expanded to address the four major modes of loading, tension-extension (TE), tension-flexion (TF), compression-extension (CE), and compression-flexion (CF), as detailed by the NHTSA.¹² The proposed neck injury criteria is referred to as N_{ij} where the i and j indices refer to one of the four major modes of loading, i.e. TE, TF, CE, or CF. The N_{ij} is defined as follows:

$$N_{ij} = \frac{F_z}{F_{\text{int}}} + \frac{M_y}{M_{\text{int}}}$$

where F_z is the axial load, F_{int} is the corresponding critical intercept value for the normalized load (3600 N for tension and compression for the 50th percentile adult male), M_y is the flexion/extension bending moment, and M_{int} is the critical incept of the corresponding moment (410 Nm for flexion and 125 Nm for extension). Based on comparisons with NCAP crashes, a critical value of 1.0 was proposed for the N_{ij} , which would correspond to a 15 percent risk of a serious injury (AIS \geq 3) for all occupant sizes. (An N_{ij} value of 1.4 theoretically corresponds to a 30 percent risk of a serious injury.)¹²

¹³ Abbreviated Injury Scale, Association for the Advancement of Automotive Medicine, Des Plaines, IL 60018.

¹⁴ Prasad P, Daniel RP. A Biomechanical Analysis of Head, Neck, and Torso Injuries to Child Surrogates Due to Sudden Torso Acceleration, SAE Paper 841656, 1984.

Segment Definition and Coordinate System

Occupant simulations in HVE assume a set of rigid bodies fixed together by mathematical representations of the joints to represent the human body. Fifteen segments are defined in the model by the HVE human editor that are connected to each other by a system of fourteen joints. The fifteen segments are illustrated in Figure 5.

The base coordinate system of the HVE human lies within the simulated pelvis of the human model. The coordinate system was established such that the positive x-axis points anteriorly. The positive y-axis points laterally to the human's right and the positive z-axis points caudally (towards the feet in a standing position). Each body segment also has a local coordinate system associated with it. The orientation of each segment coordinate system is fixed locally to the segment but may vary globally relative to the segment's position in space.

Simulation Set-up

Four simulated occupants were placed in the GATB simulation to represent several of the school bus occupants. Three of the simulated occupants were placed in row 10, on the passenger side of the bus. These simulated occupants represented two seriously injured 7 year-old females¹⁵ and a minorly injured 30 year-old male¹⁶. The two 7 year-old females were reportedly restrained by lap belts while the 30 year-old male was reportedly unrestrained. The final simulated occupant was placed in row 5, on the driver's side of the school bus. This simulated occupant represented a minorly injured 18 year-old female.¹⁷ The 18 year-old female reported wearing the available lap belt.

The GEBOD software representations of the 7 year-old females were 50th percentile 6 year-old females. The representation for the 30 year-old male was a 50th percentile adult male and the representation for the 18 year-old female was a 50th percentile adult female.

An assumption was made that the software representation of each simulated occupant would reflect the kinematics of the passengers positioned in the bus despite differences in age, height, and weight. The simulated occupant sizes were consistent throughout the position and restraint conditions and therefore, comparisons between predicted injury levels, in simulated occupants of this size, across different conditions were made.

¹⁵ Passengers #1 and 2 in the Survival Factors Group Factual Report of Investigation.

¹⁶ Passenger #41 in the Survival Factors Group Factual Report of Investigation

¹⁷ Passenger #36 in the Survival Factors Group Factual Report of Investigation.

Seating Location and Orientation

A seating chart was developed from the passenger interviews and witness statements that placed each occupant in a specific seat.¹⁸ Unfortunately, absolute accuracy of the seating chart and the orientations of the students in the seats was often difficult to achieve since the chart was based on the reports of the bus occupants and witnesses. The orientations of bus occupants, for example, whether the child was sitting next to the window or the aisle or whether the child was facing forward, or kneeling on the seat, were based on the reports of the bus passengers and witnesses. For the study, the simulated occupants were positioned in the bus based on the developed seating chart. Figure 6 diagrams the locations of the four simulated occupants placed in the bus at the beginning of the simulation, prior to impact (time = 0.00 seconds). In addition several of the bus chaperones indicated that the lap belts were not snug due to knots in the belt webbing. Belt slack was also investigated for this study.

Initial Positioning

Pelvis Location

The GATB simulated occupants were initially positioned by the location of the lower torso segment. The location of this segment for each of the occupant positions is shown in Table 1 below.

Table 1: The pelvis locations and orientations for each of the four simulated occupants referenced to the bus's center of gravity.

Seat Location	x (in)	y (in)	z (in)	Pitch (deg)
5C	-62.5	-37.0 ¹⁹	-25.6	15
10D	-198.3	8.0	-24.2	20
10E	-198.8	25.5	-21.7	25
10F	-198.8	38.5	-21.7	25

Joint Angles

The joint angles altered²⁰ from the default position are listed below. These joint orientations were consistent for each scenario. In addition, the resistance of each joint was set

¹⁸ Survival Factors Factual Report of Investigation

¹⁹ Three different lateral positions along the seat cushion were simulated. These addressed the window (37.0"), center (25.25"), and aisle seat positions (13.5"). Injury prediction values are reported for the window and center seat positions only as the aisle position resulted in greater injury and occupant motion inconsistent with the passenger's report.

²⁰ Joint angles were altered to position the occupants in a neutral seated position.

to the default level for GATB. For the simulated occupants representing the 7 year-old females, the upper arms were rotated outward by 3.5 degrees and flexed 5 degrees. The lower arms were flexed at 70 degrees. The upper legs were not outwardly rotated and were flexed at 70 degrees while the lower legs were flexed at 40 degrees. The feet were flexed at 80 degrees. For the simulated occupant representing the 18 year-old female, the upper arms were rotated outward by 15 degrees and flexed 20 degrees. The lower arms were flexed at 45 degrees. The upper legs were outwardly rotated by 5 degrees and flexed at 70 degrees while the lower legs were flexed at 70 degrees. For the simulated occupant representing the 30 year-old male, the upper arms were rotated outward by 15 degrees and flexed 20 degrees. The lower arms were flexed at 45 degrees. The upper legs were outwardly rotated by 5 degrees and flexed at 75 degrees while the lower legs were flexed at 90 degrees.

Restraint Systems

The locations of the attachments for the lap belts were based on the measurements on the accident bus that are detailed in the Survival Factors Group Factual Report of Investigation. The attachments for the shoulder harness were developed based on the height of the seat back. Both the lap and the lap-shoulder belt material properties in GATB were developed based on the default belt properties in HVE. These properties develop a simulated belt based on the linear, quadratic, and cubic stretch rates, the damping constant, the breaking strength, and the unloading slope. These belts do allow the belt to slide over the body segments, as could happen during an accident. The attachment points for both the lap and the lap-shoulder belts were theoretical attachments. Therefore, the seats were not stiffened to support the added load of the belt and an attachment for the shoulder harness was not simulated. Thus, the attachment points were not designed specifically for each bus occupant. In addition, as mentioned above, the belt slack in the lap belt restrained condition was investigated as belt slack was reported by the bus chaperones. The attachment points referenced to the center of gravity of the bus for both the lap and shoulder belts are shown in Table 2.

Table 2: The attachment points for the lap and shoulder belts placed in Row 10 of the bus.

Seat	Anchor	Lap Belts		Shoulder Belts	
		Left	Right	Left	Right
5A,B	x (in)	-203.0	-203.0		
	y (in)	-41.5	-32.5 ²¹		
	z (in)	-14.5	-14.5		
10D	x (in)	-203.0	-203.0	-206.0	-203.0
	y (in)	9.0	18.0	7.5	18.0
	z (in)	-14.5	-14.5	-44.5	-14.5
10E	x (in)	-203.0	-203.0	-203.0	-206.0

²¹ The belt attachment points for the center seat position were -30.0 (left) and -20.5 (right).

	y (in)	20.5	30.0	20.5	31.5
	z (in)	-14.5	-14.5	-14.5	-44.5
10F	x (in)	-203.0	-203.0	-203.0	-206.0
	y (in)	32.5	41.5	32.5	43.0
	z (in)	-14.5	-14.5	-14.5	-44.5

The lap/shoulder belts were designed such that the upper restraint was toward the outside of the seat for the two edge positions and was toward the window for the center position. (The belt for seat 10D wraps over the left shoulder. The belts for seats 10E and 10F wraps over the right shoulder.)

Contact Surfaces

GATB allows contact surfaces to be developed from plane surfaces only. (Occupant-to-occupant contacts are calculated based on elliptical surfaces.) The plane surface is adequate when the contact is flat into the plane of the contact surface but errors may result if the contact occurs at the edge of the plane. The resulting motion from this edge contact is dependent on a mathematical equation to determine the location of the contacting segment and the penetration into the contact surface. Therefore, flat surfaces were placed on the edges of contact surfaces, where appropriate, in an effort to avoid errors at these points.

Seat Dimensions

The dimensions of the seats were measured on the accident bus and are detailed in the Survival Factors Group Factual Report of Investigation. The spacing between seats was set according to the plan drawing provided by AmTran Corporation.²² The material properties for the seats were assigned the default seat material in HVE.

Window Dimensions

The separation between windows was set based on the plan and elevation of the bus provided by AmTran Corporation²² The material properties for the windows were developed from the default windshield material in HVE.

Occupant Kinematics: Adjacent to Side Emergency Exit Door

The simulated occupant motion for the occupant located in seat 5C, the seat adjacent to the side emergency exit door, was such that the occupant moved away from the side emergency exit door in both the unrestrained and lap belt restrained conditions. In the unrestrained condition, the initial impact was with the seat back in front followed by motion into or towards

²² AmTran Corporation Conway, AR 72033.

the aisle, depending on the simulated occupant’s initial seating position. Impact with the unprotected handles and hardware of the side emergency exit door during the primary impact was not predicted in this simulation. Furthermore, the simulated occupant motion indicated that the simulated occupant moved away from the unprotected area even after the initial impact. In the restrained condition, the initial motion was again forward and lateral toward the right. Due to the action of the lap belt, the simulated occupant did not contact the seat back in front but rather impacted the seat cushion as the upper body rotated about the fixed pelvis. The simulated occupant traveled farther into the aisle when placed in the center seat position and did have some contact with the adjacent seat cushion. Injuries were only predicted for the center seat position in the lap belted condition. (The actual injuries sustained were a left wrist strain and a thumb fracture.)

The predicted injury values for both the unrestrained and lap belt restrained conditions are shown in Table 3 below for both the center and window seat positions.

Table 3: The predicted injury values for the simulated occupant in row 5 on the driver’s side of the bus near the side emergency exit door. Both the window and center seat position injury values are shown in the unrestrained and lap belt restrained conditions.

Position	HIC	Chest Accel. (G)	Neck Flexion (Nm)	Neck Extension (Nm)
Center, Unbelted	360	47	12	9
Center, Lap Belted	2120	25	265	31
Window, Unbelted	150	43	6	15
Window, Lap Belted	810	20	24	56

Occupant Kinematics: Row 10

Scenario 1: Lap-belt restrained simulated 7 year-old females with unrestrained simulated adult male

Scenario 1 represents the condition where the two simulated occupants, representing the 7-year-old females, were restrained with lap belts while the simulated adult male was unrestrained. In addition, based on the statements of the adult male, there was some amount of slack in the belts at the time of the accident. Therefore, the slack in the belts was varied to better understand the occupant motion and predicted injury levels. Three main belt slack amounts were investigated: no slack (0 inches), 1 inch of belt slack, and 2 inches of belt slack. The simulation results indicated that the simulated occupant closest to the window (10F) impacted that window and the sidewall. The simulated occupant in seat 10E traveled forward of the simulated occupant in 10F and then contacted the sidewall and the window. In addition, head and body contact occurred between these two simulated occupants. The simulated occupant in seat 10D traveled farther forward than the other two simulated occupants due to the lack of a restraint. This simulated occupant collided with the other two simulated occupants

and pushed the simulated occupant in 10E farther forward. These general trends were seen for each amount of belt slack although the more slack that was present in the belts, the farther forward the two restrained simulated occupants traveled, as expected. The predicted injury values are shown in Figure 7 through Figure 10 for the head, chest, and neck.

Table 4 indicates the actual injuries sustained by the passengers in seats 10D, 10E, and 10F on the school bus. The passenger in 10F was more injured than the passenger in seat 10E, yet the predicted injuries discussed above indicate the opposite. Thus, another combination of belt slack was investigated where the simulated occupant in seat 10F had 2 inches of belt slack while the simulated occupant in seat 10E had no slack in the belt. The basis for this combination was to prevent the simulated occupant in the center position from being impacted by the larger simulated occupant in seat 10D. Figure 7 through Figure 10 also show the predicted injury levels for this combination of belt slack. The simulated occupants in seats 10E and 10D were predicted to sustain head injury in this condition. All three simulated occupants were predicted to sustain chest injuries in this condition. Neck injuries in flexion and extension were not predicted for this condition.

Although the predicted injury patterns do not exactly match the actual sustained injuries, the trends are still evident. Furthermore, the discrepancy between the predicted injuries and the actual injuries is believed to result from an inability to simulate the damage to the bus sidewall and window in this region of the bus, which was the area of maximum intrusion. Therefore, the simulated occupant in seat 10F impacted a smooth flat sidewall and window, when in reality those surfaces were deforming toward the occupants in row 10 on the passenger side of the school bus. In addition, the intrusion into the sidewall of the bus would have reduced the travel distance for the other two occupants on the seat making it more likely that those occupants would impact other occupants rather than traveling forward and impacting the sidewall. Figure 11 shows a close-up view of the damage to the bus sidewall in this area. Therefore, the injuries to the two simulated occupants not along the wall may have been reduced. This is a current limitation of the simulation software.

The following scenarios represent hypothetical cases in which all occupants were unrestrained, restrained by lap belts, or restrained by lap/shoulder belts. In addition, the final scenario looks at the predicted injury levels if the simulated occupants in seat 10E and 10F were alone on the seat.

Scenario 2: All three simulated occupants unrestrained

In the condition where all three simulated occupants in Row 10, on the passenger side, were unrestrained, all three impacted the right sidewall and windows. The simulated occupant in seat 10F was the first to impact the sidewall. Then the simulated occupant in seat 10E impacted the first simulated occupant and rotated forward into the sidewall and window. The simulated occupant in seat 10D, the 50th percentile male, traveled diagonally toward the right, impacting the seat back in front with the upper and lower legs and also with the upper body. This simulated occupant then impacted the center seated simulated occupant and the sidewall

and windows. The predicted injury levels are shown in Figure 12 through Figure 15. Only the simulated occupant in seat 10E was predicted to sustain a head injury during the unrestrained condition. All three simulated occupants were predicted to sustain chest injuries in the unrestrained condition. Neck injuries in flexion and extension were not predicted for the unrestrained condition.

Scenario 3: All three simulated occupants lap belt restrained

Occupant motion for the condition where all three simulated occupants were restrained by lap belts was similar as to that seen for the condition where two of the simulated occupants were restrained while the third was not (scenario 1). The differences were seen with the simulated occupant in seat 10D who did not travel as far forward and impacted the simulated occupant in the center seat more with the upper body, as the lower body was restrained. This simulated occupant's head still contacted the sidewall and window but the impact was not distributed across the entire body as in the unrestrained condition. Therefore, the predicted HIC value was higher for the simulated occupant in seat 10D for scenario 3 than for scenario 2 but the HIC value was not as high as for scenario 1. Again, these predicted injury levels are shown in Figure 12 through Figure 15.

Head injuries were predicted for the simulated occupants in seats 10E and 10D. All three simulated occupants were predicted to sustain chest injuries in the lap belt restrained condition although the chest acceleration values were lower than those in the unrestrained condition. Neck injuries in flexion and extension were not predicted for the lap belt restrained condition.

Scenario 4: All three simulated occupants lap/shoulder belt restrained

The occupant motion for the condition where all three simulated occupants were restrained by lap/shoulder belts was similar to the condition where all three were restrained by lap belts (scenario 3). Due to the configuration of the shoulder harness for seat 10D, with the belt wrapping toward the left shoulder, the upper body slid from the restraint during the forward and lateral motion toward the right. The predicted injuries were almost identical to those for the condition described in scenario 3. Again, these predicted injury levels are shown in Figure 12 through Figure 15.

Head injuries were predicted for the simulated occupants in seats 10E and 10D. All three simulated occupants were predicted to sustain chest injuries in the lap/shoulder belt restrained condition although the chest acceleration values were again lower than those in the unrestrained condition. Neck injuries in flexion and extension were not predicted for the lap/shoulder belt restrained condition.

Scenario 5: Unrestrained and Lap restrained 7 year-old females without adult male

In this scenario, the two simulated occupants representing the 7-year-old females were placed alone on the seat. (The simulated occupant representing the adult male was not included in this scenario.) The occupant motion for the two simulated occupants was similar for both the unrestrained and lap belt restrained conditions. The main difference was that the two simulated occupants were not impacted by the third simulated occupant as in the other scenarios. In both cases, unrestrained and lap belt restrained, the HIC values were lower than for the other scenarios where the adult male was present. The predicted chest injuries for the simulated occupant in seat 10F were similar to those seen in scenarios 2 and 3. Contrarily, the predicted chest injuries for the simulated occupant in seat 10E were less than those seen in the other scenarios. The predicted neck injuries were again generally lower than seen in the other scenarios except for the simulated occupant in seat 10E while restrained by a lap belt. In that condition, the predicted neck extension moments were greater than seen in the previous scenarios but were still below the injury assessment reference values. The predicted injury values are again shown in Figure 12 through Figure 15 for comparison to the injury values in the previous scenarios.

A photographic time history of the occupant motion for the simulated occupants in row 10 on the passenger side of the bus is shown in Figure 16.

Summary

A summary of the predicted injuries listed above is displayed in Table 4 below. A check mark (v) indicates the prediction of an injury to that segment of the simulated occupant's body, based on the simulation. In addition, the actual injuries to the bus occupants are summarized in Table 4 and are detailed in Table 5.

Table 4: A summary of the predicted injuries to the simulated occupants based on the simulation of the bus and also the sustained injuries to the true bus passengers (see Table 5). (A v next to the seating location indicates that the occupant was predicted to sustain an injury.)

Seating Location	Segment	Unrest. And Lap Belt Restrained (2", 0")	Unrest. Only	Lap Belt Only	Lap-Shoulder Belt	Alone on Seat (Unrest.)	Actual Injuries
Seat 5C	Head Thorax Neck	N/A		v ²³ v	N/A	N/A	
Seat 10D	Head Thorax Neck	v v	v	v v	v v	N/A	
Seat 10E	Head Thorax	v v	v v	v v	v v	v	v

²³ Injuries were not predicted for the lap belted restrained condition when the simulated occupant was seated along the window.

	Neck						
Seat 10F	Head						v
	Thorax	v	v	v	v	v	v
	Neck						v

Actual Reported Injuries

A summary of the injuries sustained by the occupants in the accident is detailed below by seating position. This information was taken from the Survival Factors Factual Report.

Table 5: The injuries sustained by the bus occupants as reported in the Survival Factors Factual Report.

Seat	Injury	Injury Codes ²⁴
5C (#36)	An 18-year-old female sustained a left wrist sprain and thumb fracture.	Minor
10D (#41)	A 30-year-old male sustained a right eyebrow laceration and facial abrasions.	Minor
10E (#2)	A 7-year-old female sustained an open right tibia/fibula fracture, left closed tibia/fibula fracture, small liver laceration, forehead abrasion, back abrasion, and front tooth injury.	Serious
10F (#1)	A 7-year-old female sustained right frontal and right cerebellar contusions, a C-7 transverse spinous process fracture, right clavicular lateral fracture, and a small non-displaced right pubic rami fracture.	Serious

Submitted by:

Kristin M. Bolte, Ph.D.
Mechanical/Biomechanical Engineer

²⁴ 49 CFR 830.2 defines a fatal injury as: any injury which results in death within 30 days of the accident. A serious injury as: an injury which requires hospitalization for more than 48 hours, commencing within seven days from the date the injury was received; results in a fracture of any bone (except simple fractures of the fingers, toes, or nose); causes severe hemorrhages, nerve, muscle, or tendon damage; involves any internal organ; or involves second or third degree burns, or any burns affecting more than 5 percent of the body surface.



Figure 1: The final rest locations of the school bus and dump truck.



Figure 2: The exterior damage to the school bus.

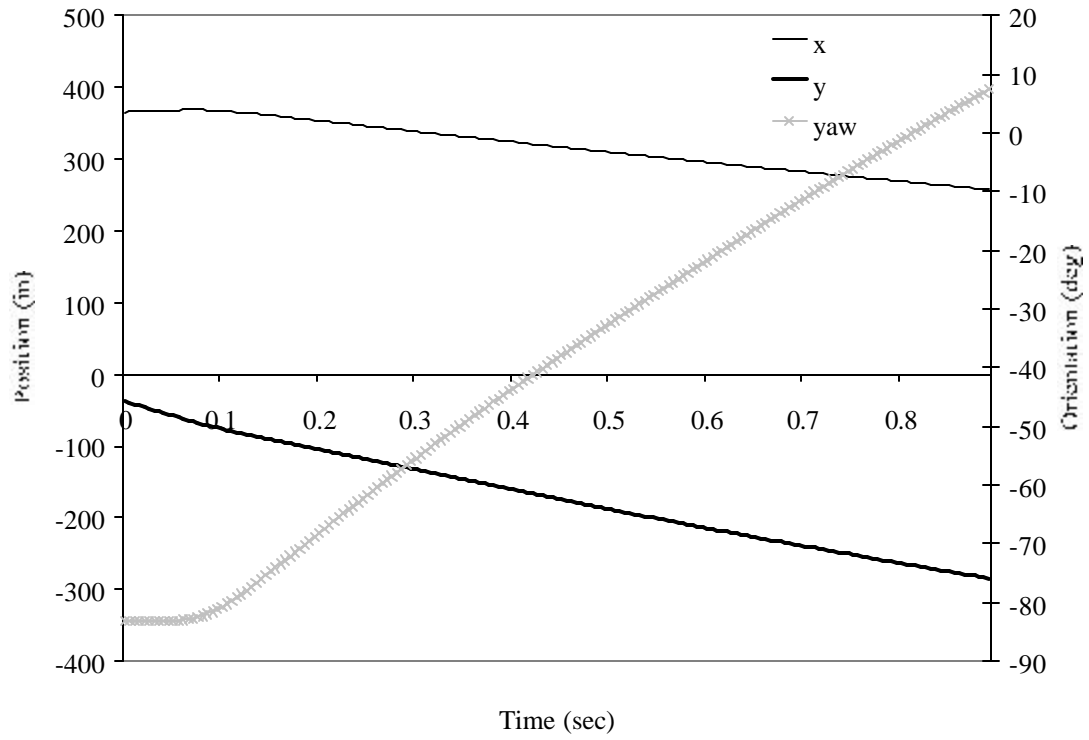


Figure 3: The position and orientation time history of the bus as calculated from HVE using EDSMAC4. This information was input into GATB in order to determine the occupant kinematics.

a.



b.



Figure 4: Photographs showing the interior damage a. down the length of the bus and b. in the area of impact.

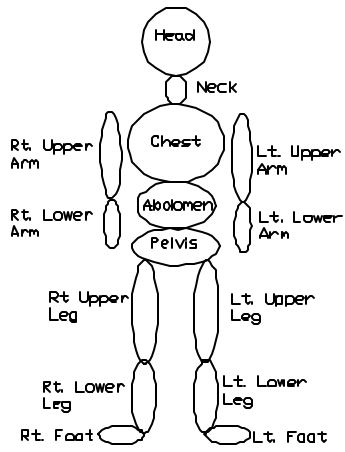
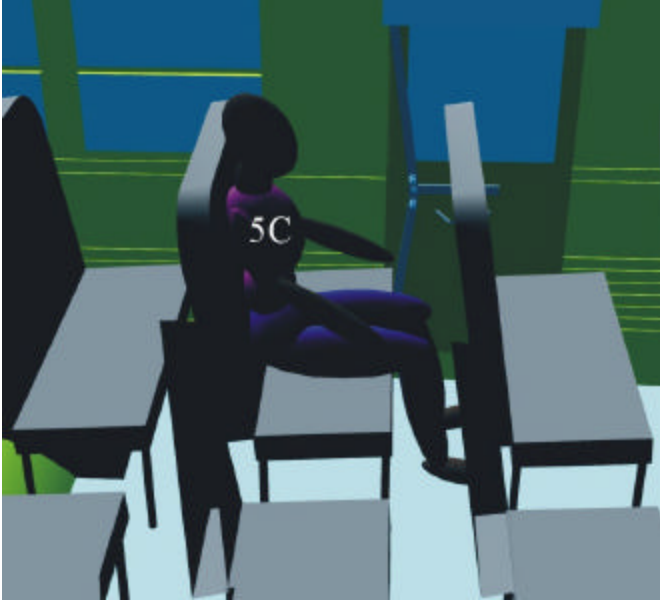


Figure 5: The fifteen body segments of the HVE Human Model.

a.



b.



Figure 6: The initial position (a) for the simulated occupant in row 5 on the driver's side of the bus near and the emergency exit door (note orientation of door not to scale) and the initial positions (b) for the simulated occupants in row 10 on the passenger side of the bus.

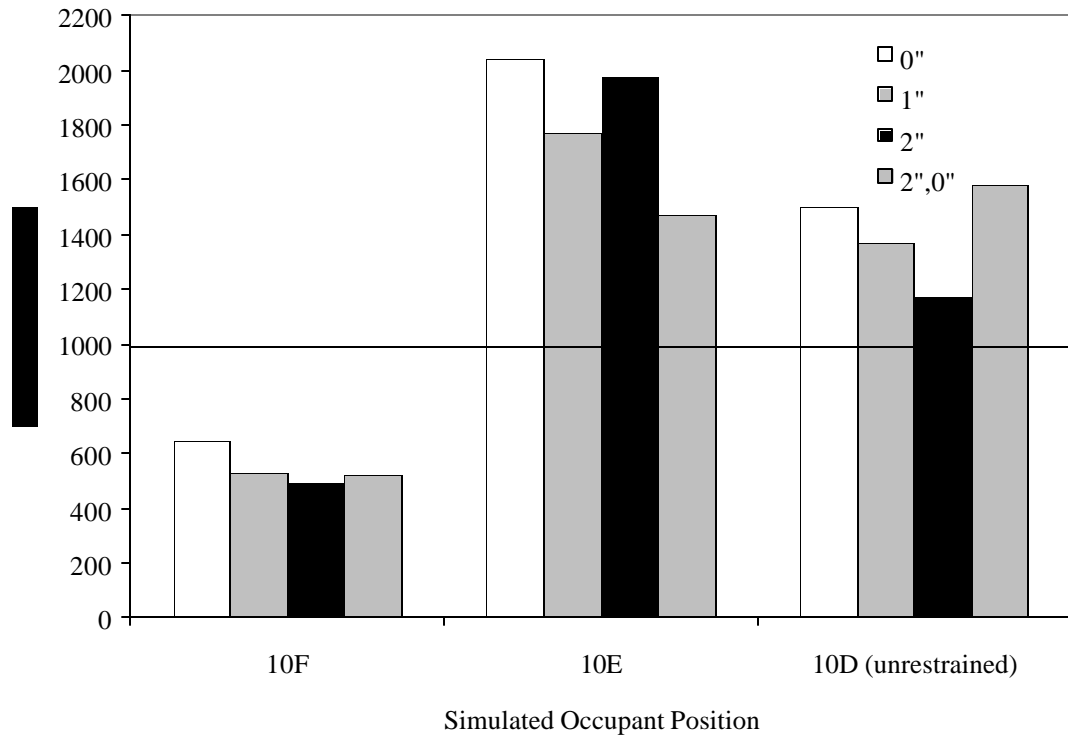


Figure 7: A comparison of the predicted HIC values for the simulated occupants in Row 10 on the passenger side of the school bus. Four different conditions are represented. In each of the four conditions two of the simulated occupants are lap belt restrained (10F and 10E) while the third simulated occupant (10D) is unrestrained. The four conditions represent the amount of belt slack present in each of the lap belt systems varying between no belt slack (0"), 1" belt slack, 2" belt slack, and 2" belt slack for position 10F and 0" belt slack for position 10E. The critical HIC value is 1000 for predicting risk of skull fracture ($AIS \geq 2$).

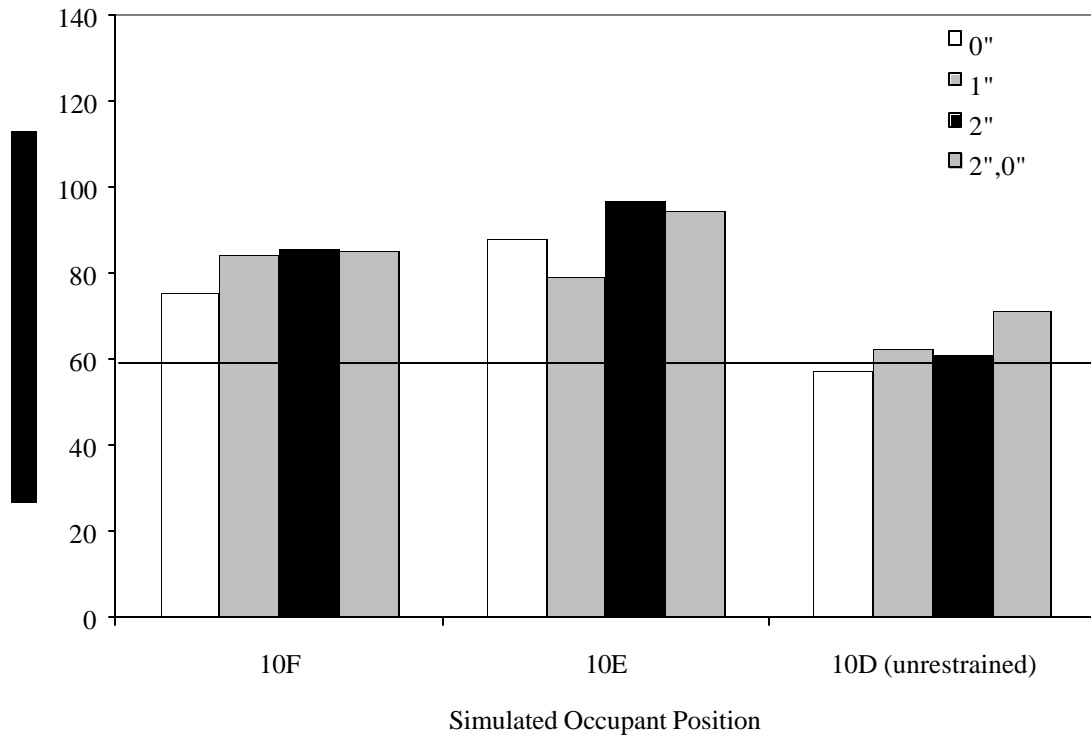


Figure 8: A comparison of the predicted chest acceleration values for the simulated occupants in Row 10 on the passenger side of the school bus. Four different conditions are represented. In each of the four conditions two of the simulated occupants are lap belt restrained (10F and 10E) while the third simulated occupant (10D) is unrestrained. The four conditions represent the amount of belt slack present in each of the lap belt systems varying between no belt slack (0"), 1" belt slack, 2" belt slack, and 2" belt slack for position 10F and 0" belt slack for position 10E. The critical chest acceleration value is 60 g for predicting risk of chest injury.

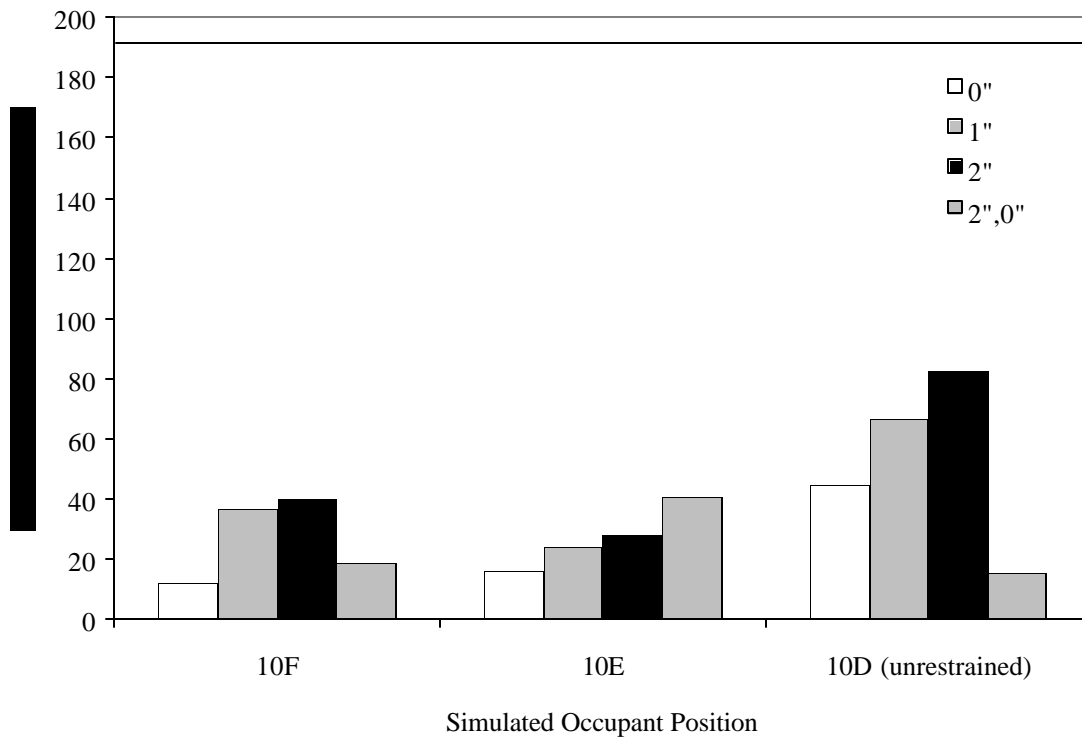


Figure 9: A comparison of the predicted neck flexion values for the simulated occupants in Row 10 on the passenger side of the school bus. Four different conditions are represented. In each of the four conditions two of the simulated occupants are lap belt restrained (10F and 10E) while the third simulated occupant (10D) is unrestrained. The four conditions represent the amount of belt slack present in each of the lap belt systems varying between no belt slack (0"), 1" belt slack, 2" belt slack, and 2" belt slack for position 10F and 0" belt slack for position 10E. The critical value for neck flexion is 190 Nm.

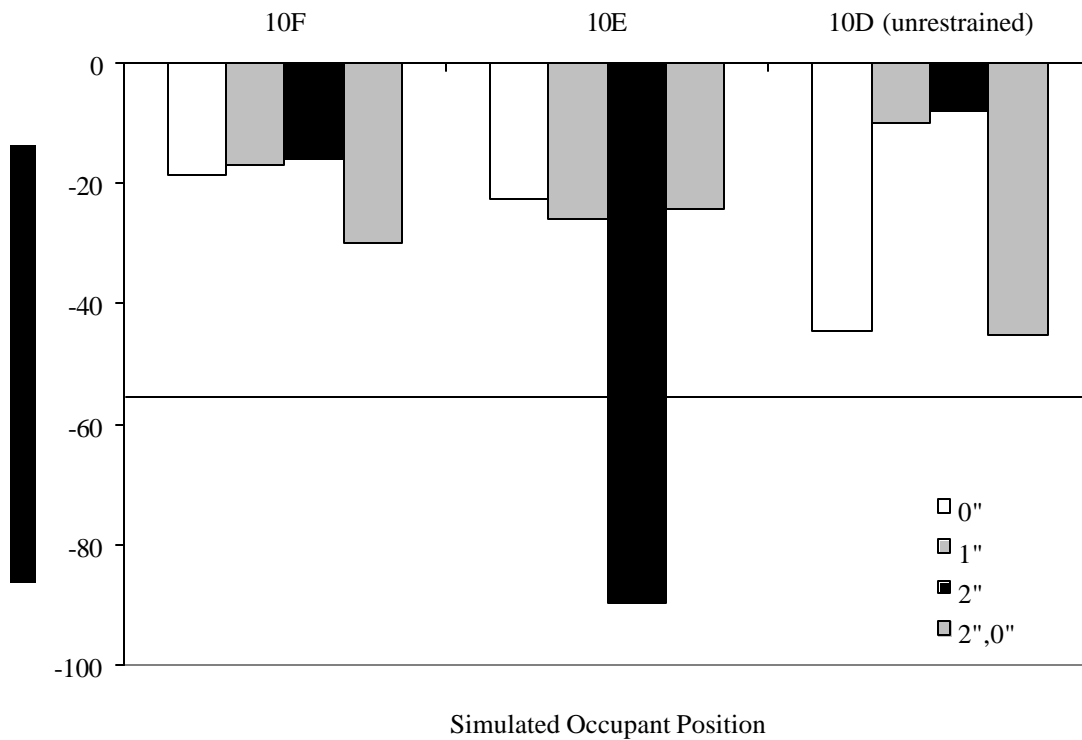


Figure 10: A comparison of the predicted neck extension values for the simulated occupants in Row 10 on the passenger side of the school bus. Four different conditions are represented. In each of the four conditions two of the simulated occupants are lap belt restrained (10F and 10E) while the third simulated occupant (10D) is unrestrained. The four conditions represent the amount of belt slack present in each of the lap belt systems varying between no belt slack (0"), 1" belt slack, 2" belt slack, and 2" belt slack for position 10F and 0" belt slack for position 10E. The critical value for neck extension is 57 Nm.



Figure 11: A close-up view of the damage to the bus sidewall on the passenger's side of the bus near the last rows of the bus.

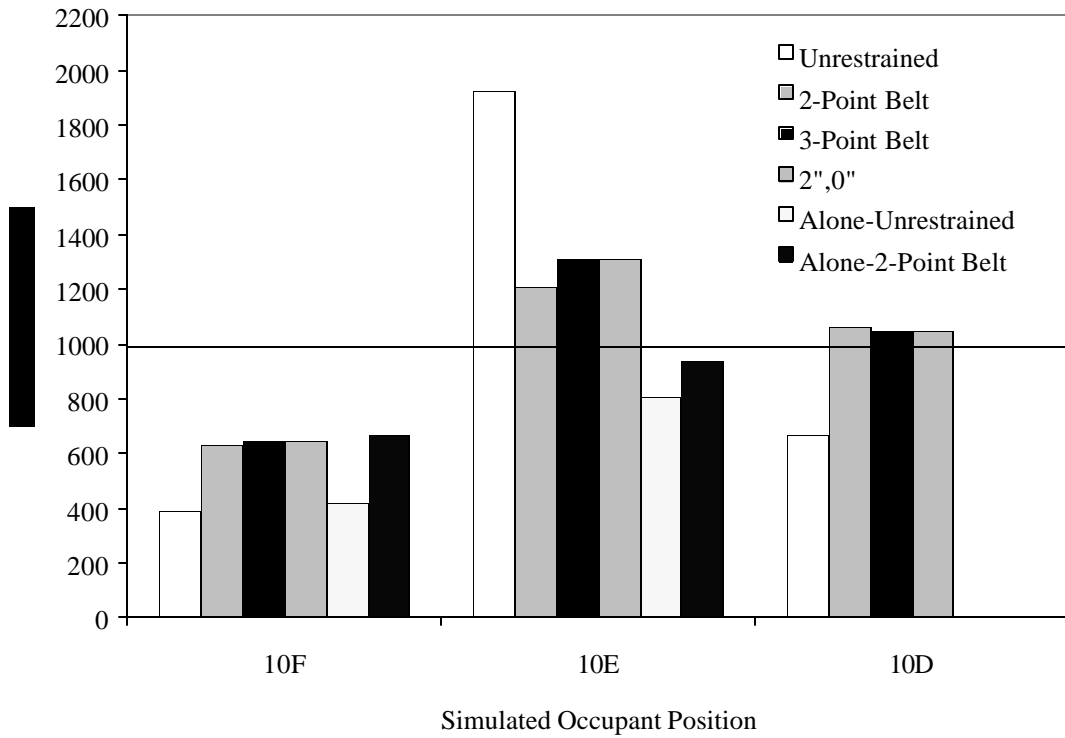


Figure 12: A comparison of the predicted HIC values for the simulated occupants in Row 10 on the passenger side of the school bus. Six different conditions are represented. Those conditions are when all three simulated occupants are (1) unrestrained, (2) lap belt restrained, and (3) lap/shoulder belt restrained, the condition when (4) two of the simulated occupants are lap belt restrained and one simulated occupant is unrestrained and the condition when two simulated occupants are alone on the seat (5) unrestrained and (6) lap belt restrained. The critical HIC value is 1000 for predicting risk of skull fracture ($AIS \geq 2$).

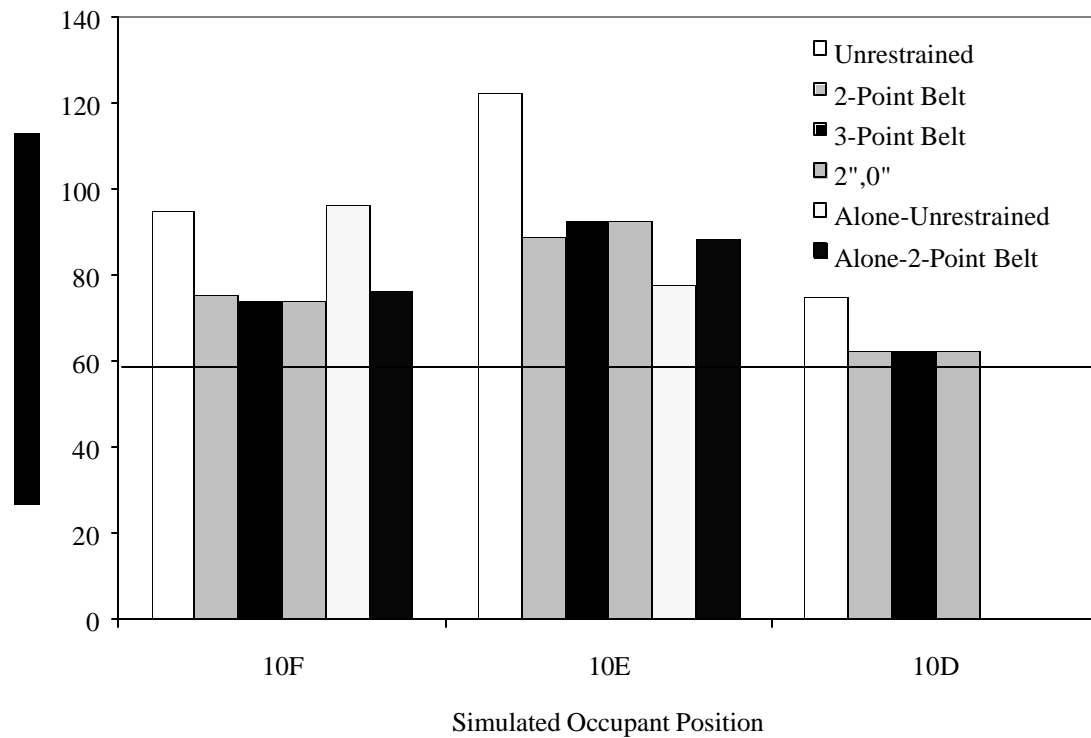


Figure 13: A comparison of the predicted chest acceleration values for the simulated occupants in Row 10 on the passenger side of the school bus. Six different conditions are represented. Those conditions are when all three simulated occupants are (1) unrestrained, (2) lap belt restrained, and (3) lap/shoulder belt restrained, the condition when (4) two of the simulated occupants are lap belt restrained and one simulated occupant is unrestrained and the condition when two simulated occupants are alone on the seat (5) unrestrained and (6) lap belt restrained. The critical chest acceleration value is 60 g for predicting risk of chest injury.

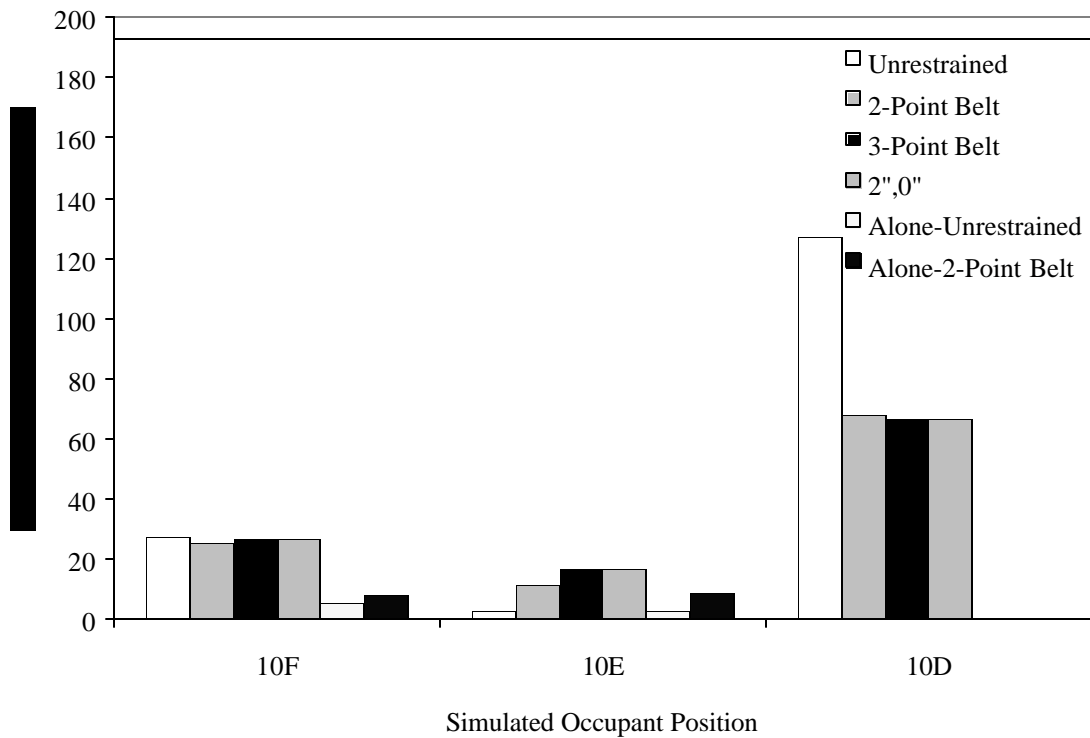


Figure 14: A comparison of the predicted neck flexion values for the simulated occupants in Row 10 on the passenger side of the school bus. Six different conditions are represented. Those conditions are when all three simulated occupants are (1) unrestrained, (2) lap belt restrained, and (3) lap/shoulder belt restrained, the condition when (4) two of the simulated occupants are lap belt restrained and one simulated occupant is unrestrained and the condition when two simulated occupants are alone on the seat (5) unrestrained and (6) lap belt restrained. The critical value for neck flexion is 190 Nm.

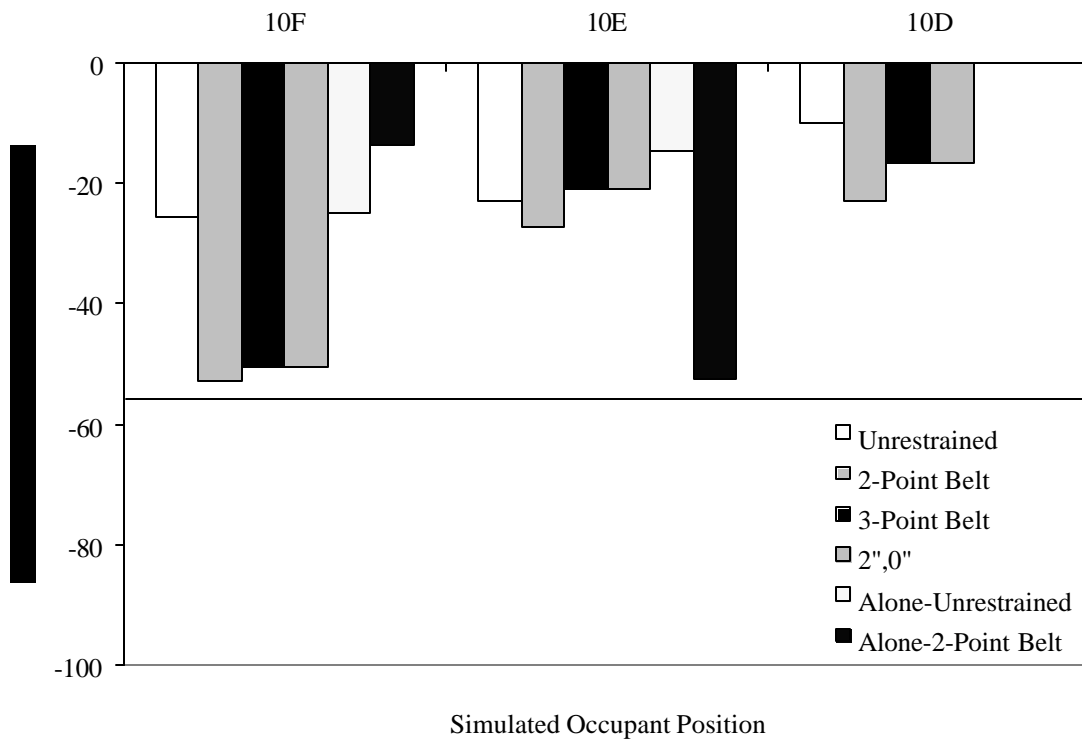


Figure 15: A comparison of the predicted neck extension values for the simulated occupants in Row 10 on the passenger side of the school bus. Six different conditions are represented. Those conditions are when all three simulated occupants are (1) unrestrained, (2) lap belt restrained, and (3) lap/shoulder belt restrained, the condition when (4) two of the simulated occupants are lap belt restrained and one simulated occupant is unrestrained and the condition when two simulated occupants are alone on the seat (5) unrestrained and (6) lap belt restrained. The critical value for neck extension is 57 Nm.

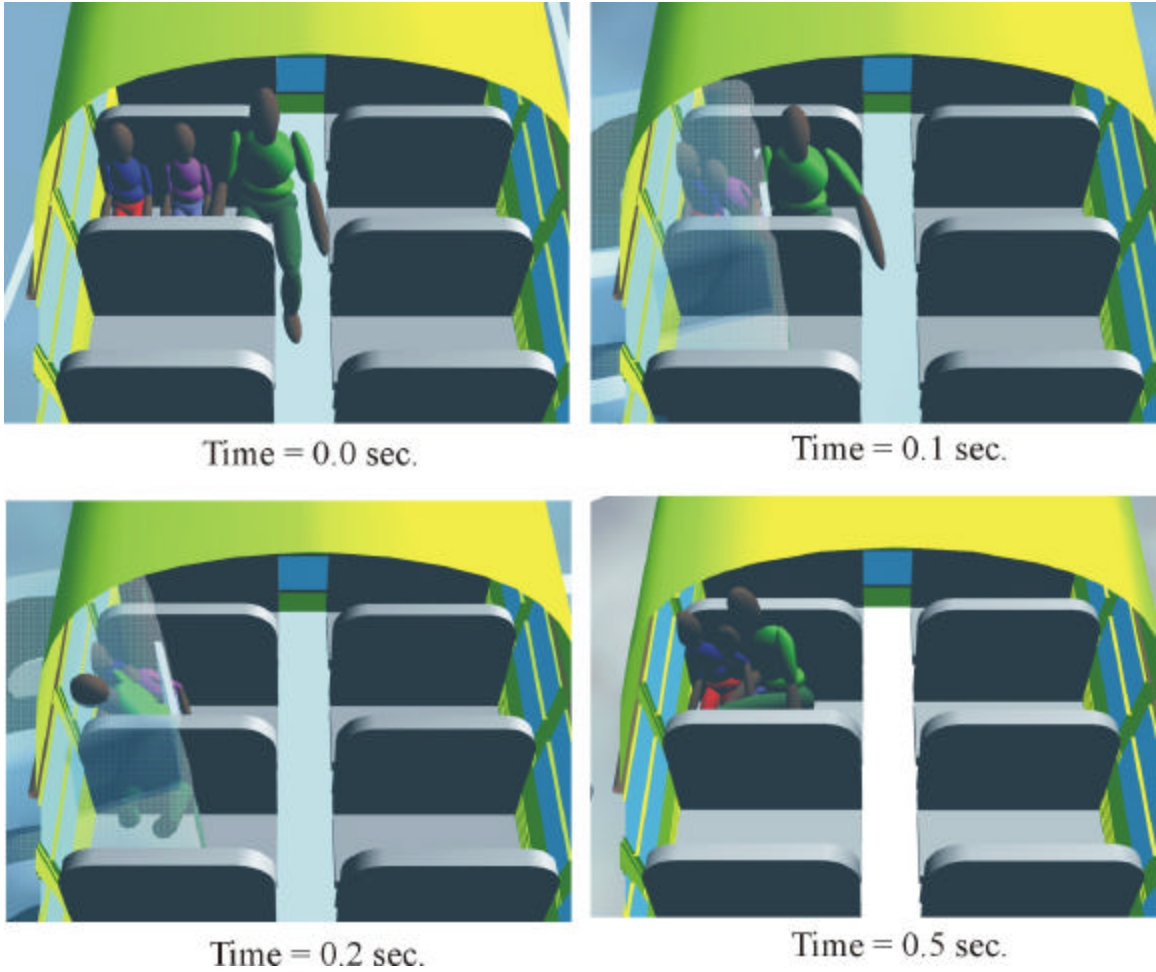


Figure 16: A time-history of the occupant kinematics simulation in the scenario where two simulated occupants are lap belt restrained while the third is unrestrained. The time reference is based on impact at 0.0 seconds. (Note other occupants were in this region of the bus but were not included in the simulation. Furthermore, the deformation was not simulated but the simulated intrusion can be seen with the semi-transparent dump truck.)